Predetermined recruitment of calcium release sites underlies excitation–contraction coupling in rat atrial myocytes

Lauren Mackenzie*, Martin D. Bootman*†, Michael J. Berridge*† and Peter Lipp*

**Laboratory of Molecular Signalling, The Babraham Institute, Babraham, Cambridge CB2 4AT and †Department of Zoology, University of Cambridge, Downing Street, Cambridge CB2 3EJ, UK*

(Received 30 June 2000; accepted after revision 2 October 2000)

1. Excitation–contraction coupling (E–C coupling) was studied in isolated fluo-3-loaded rat atrial myocytes at 22 and 37 °C using rapid confocal microscopy.

2. Within a few milliseconds of electrical excitation, spatially discrete subsarcolemmal Ca^{2+} signals were initiated. Twenty to forty milliseconds after stimulation the spatial overlap of these Ca^{2+} signals gave a 'ring' of elevated Ca^{2+} around the periphery of the cells. However, this ring was not continuous and substantial Ca^{2+} gradients were observed.

3. The discrete subsarcolemmal Ca^{2+}-release sites, which responded in a reproducible sequence to repetitive depolarisations and displayed the highest frequencies of spontaneous Ca^{2+} sparks in resting cells, were denoted 'eager sites'.

4. Immunostaining atrial myocytes for type II ryanodine receptors (RyRs) revealed both subsarcolemmal 'junctional' RyRs, and also 'non-junctional' RyRs in the central bulk of the cells. A subset of the junctional RyRs comprises the eager sites.

5. For cells paced in the presence of 1 mM extracellular Ca^{2+}, the response was largely restricted to a subsarcolemmal 'ring', while the central bulk of the cell displayed a ~5-fold lower Ca^{2+} signal. Under these conditions the non-junctional RyRs were only weakly activated during E–C coupling. However, these channels are functional and the Ca^{2+} stores were at least partially loaded, since substantial homogeneous Ca^{2+} signals could be stimulated in the central regions of atrial myocytes by application of 2·5 mM caffeine.

6. Neither the location nor activation order of the eager sites was affected by increasing the trigger Ca^{2+} current (by increasing extracellular Ca^{2+} to 10 mM) or the sarcoplasmic reticulum (SR) Ca^{2+} load (following 1 min incubation in 10 mM extracellular Ca^{2+}), although with increased SR Ca^{2+} load, but not greater Ca^{2+} influx, the delay between the sequential activation of eager sites was reduced. In addition, increasing the trigger Ca^{2+} current or the SR Ca^{2+} load changed the spatial pattern of the Ca^{2+} response, in that the Ca^{2+} signal propagated more reliably from the subsarcolemmal initiation sites into the centre of the cell. Due to the greater spatial spread of the Ca^{2+} signals, the averaged global Ca^{2+} transients increased by ~500 %.

7. We conclude that rat atrial myocytes display a predetermined spatiotemporal pattern of Ca^{2+} signalling during early E–C coupling. A consistent set of eager Ca^{2+} release sites with a fixed location and activation order on the junctional SR serve to initiate the cellular response. The short latency for activation of these eager sites suggests that they reflect clusters of RyRs closely coupled to voltage-operated Ca^{2+} channels in the sarcolemma. Furthermore, their propensity to show spontaneous Ca^{2+} sparks is consistent with an intrinsically higher sensitivity to Ca^{2+}-induced Ca^{2+} release. While the subsarcolemmal Ca^{2+} response can be considered as stereotypic, the central bulk of the cell grades its response in direct proportion to cellular Ca^{2+} load and Ca^{2+} influx.

In the heart, release of Ca^{2+} from the sarcoplasmic reticulum (SR) is the key event linking membrane depolarisation and mechanical activity during excitation–contraction coupling (E–C coupling) (Bers, 1991; Callewaert, 1992). It is generally accepted that Ca^{2+} influx via voltage-operated Ca^{2+} channels (VOCCs) is the major source for trigger Ca^{2+}, which subsequently activates ryanodine receptors (RyRs) in the membrane of the SR by a process known as Ca^{2+}-induced Ca^{2+} release (CICR; Fabiato, 1985). RyRs occur in clusters that give rise to localised Ca^{2+} release events denoted 'Ca^{2+} sparks' (Cheng *et al.* 1993; Lipp & Niggli, 1994). Spatiotemporal recruitment of Ca^{2+} sparks underlies the global Ca^{2+} signals that subsequently activate myocyte contraction (López-López *et al.* 1995; for review see Bootman & Berridge, 1995; Lipp & Niggli, 1996; Berridge *et al.* 1998, 1999, 2000). In ventricular myocytes, a network of tubular membranes oriented transversely to the long axis of the myocyte ('t-tubules') conduct the action potential deep within the cells. As a result, Ca^{2+} spark sites throughout the cell are activated during the action potential ensuring a spatially and temporally homogeneous Ca^{2+} rise (Cannell *et al.* 1994; Lipp *et al.* 1996*b*). In contrast, atrial myocytes do not possess a t-tubule system (Hüser *et al.* 1996; Lipp *et al.* 1996*a*, *b*), and the coupling between Ca^{2+} channels on the sarcolemma and 'junctional' RyRs on the SR occurs around the periphery of the cell (Lipp *et al.* 1990; Berlin, 1995; Lewis Carl *et al.* 1995; Hüser *et al.* 1996). Previous studies have indicated that the Ca^{2+} rise in atrial myocytes occurs initially in the subsarcolemmal region, followed by a variable degree of propagation of the Ca^{2+} signal into deeper layers of the atrial myocyte (Lipp *et al.* 1990; Berlin, 1995; Hüser *et al.* 1996). Since RyRs are present at seemingly equal abundance throughout atrial myocytes (Lewis Carl *et al.* 1995; Lipp *et al.* 2000) it is surprising that CICR can largely fail in deeper layers of the cell.

Although it has been shown that E–C coupling in atrial myocytes is initiated in the subsarcolemmal region, the precise spatiotemporal pattern of the Ca^{2+} rise has not been investigated so far. In the present study, we used rapid confocal microscopy to probe the development of the Ca^{2+} signal in the subsarcolemmal and central regions of single electrically paced atrial myocytes. Our data indicate that within the subsarcolemmal and central regions of an atrial myocyte Ca^{2+} release sites can show markedly different latencies and levels of regenerativity. The consequence is that atrial myocytes have a predetermined microscopic activation sequence of Ca^{2+} spark sites whereby single cells produce reproducible inhomogeneous Ca^{2+} increases upon depolarisation.

METHODS

Cell isolation

Atrial myocytes were isolated using established methods (Lipp *et al.* 2000). Briefly, male Wistar rats (~200 g) were killed by cervical dislocation after CO_2 anaesthesia. The hearts were quickly removed, and perfused with an extracellular solution containing (mM): NaCl, 135; KCl, 5·4; $MgCl_2$, 2; Hepes, 10; glucose, 10; pH 7·35 and 1 mg ml^{-1} collagenase (Worthington). The atria or ventricular parts were excised and gently shaken in the perfusion solution to release isolated cells.

Confocal Ca^{2+} imaging

Myocytes were adhered to poly-D-lysine-coated (Sigma) coverslips for up to 2 h before use. The cells were loaded with 2 μM fluo-3 AM for 30 min followed by an additional 30 min period for de-esterification, and then subsequently transferred to the stage of a laser scanning confocal microscope (NORAN Oz, Bicester, UK). Fluo-3 was excited at 488 nm and the emitted fluorescence was collected at wavelengths $>$ 505 nm. The confocal slit aperture was set so that the confocal plane was $<$ 1 μm in thickness. Two dimensional confocal images (frame size: 512 × 115 pixels) were acquired at 120 Hz, and line scans were performed at 10 kHz (i.e. 0·1 ms per line). Analysis of the images was conducted off-line using a modified version of NIH Image (NIH, Bethesda, USA). The myocytes were stimulated with 40 V pulses (2 ms duration) using two field electrodes (distance 0·5 cm). The stimulation frequency was set to 1 Hz for all experiments. This resulted in electrically induced Ca^{2+} transients with a constant amplitude throughout the train of stimulations (10 stimulations per train). Intracellular Ca^{2+} concentrations were calculated using a self-ratio method as originally described by Minta and co-workers (Minta *et al.* 1989). The confocal images shown represent self ratios, where every confocal frame of the sequence was normalised by an average resting cell section. All experiments were performed at room temperature (20–22°C) unless stated otherwise. During the experiments, cells were maintained in the same extracellular medium as used for cell isolation, except that collagenase was omitted and 1 or 10 mM $CaCl_2$ was added.

Calculation of time delays

Although the activation sequence of eager sites was reproducible, we attempted to quantify the temporal delay for each site. Since the synchronisation between the confocal microscope and the electrical stimulation was not perfect (we observed jitter in the range of one frame; 8 ms), we deferred to calculating relative delays, whereby all responses were normalised to that 'eager' site which consistently activated first. For this, we calculated the relative time each local Ca^{2+} transient took to reach 10% of its maximal amplitude by interpolating linearly between the data points. The use of the 10% value avoided problems with Ca^{2+} diffusion from out-of-focus release sites.

Immunocytochemistry

Rat atrial and ventricular myocytes adhered to coverslips were fixed with 4% paraformaldehyde for 1 h at room temperature. The immunocytochemical staining was performed using established methods (Sugiyama *et al.* 1994; Lipp *et al.* 2000) with a RyR type II specific monoclonal antibody (V. Sorrentino, Siena, Italy). The subcellular distribution of fluorescein-conjugated secondary antibodies was examined using an UltraView confocal microscope (Perkin Elmer Life Sciences, Cambridge, UK).

RESULTS

Depolarisation of fluo-3-loaded rat atrial myocytes resulted in spatially inhomogeneous Ca^{2+} transients. A typical example of the spatiotemporal pattern of Ca^{2+} rise following field stimulation of an atrial myocyte at 22°C and incubated in 1 mM extracellular Ca^{2+} concentration is illustrated in Fig. 1*Aa*. The sequences of images show that the Ca^{2+} signal

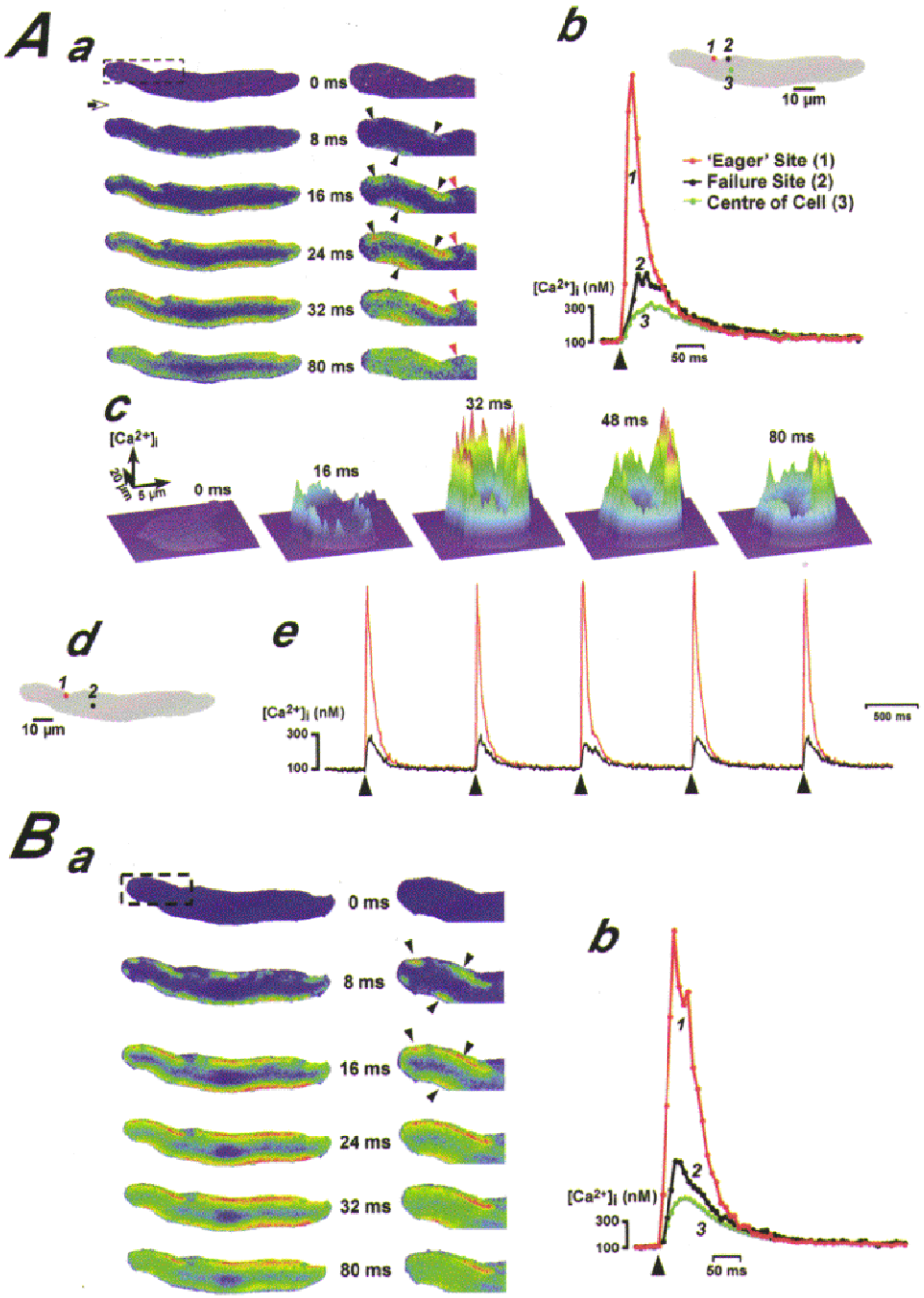

Figure 1. E–C coupling in rat atrial myocytes is characterised by inhomogeneous Ca^{2+} signals

A and *B* show the development of the depolarisation-induced Ca^{2+} responses at 20 and 37 °C, respectively. The left columns in *Aa* and *Ba* show self-ratio colour-coded images of the entire cell, and the right columns show the part of the cell bounded by the dashed box at a higher magnification. Cool colours (e.g. blue and green) indicate low Ca^{2+} concentrations and warm colours (e.g. red and yellow) denote higher Ca^{2+} concentrations. The times at which the images were taken are indicated between the columns, and the time at which the electrical pulse was applied is shown by the open arrow. Three identified 'eager' Ca^{2+} spark sites are marked by black arrowheads in *Aa* and *Ba*, and a failure site is denoted by the red arrowhead in *Aa*. The traces in *Ab* depict the time course of Ca^{2+} changes at the three subcellular sites (~1 μm in diameter) shown on the inset cell image. The same cellular regions were analysed for the traces in *Bb*. The surface plots in *Ac* depict the spatial and temporal development of the Ca^{2+} signal. The Ca^{2+} concentration is encoded by both the colour and the height of the surface. *Ad* and *Ae* illustrate that the limited Ca^{2+} response in the central region of the cell was consistently observed during a train of depolarisations (at 1 Hz). The red and black coloured traces in *Ae* show the Ca^{2+} responses observed at the correspondingly coloured regions marked in *Ad*. The timing of the electrical depolarisations is indicated by the arrowheads in *Ae*.

was more rapid in onset and more substantial in the subsarcolemmal region than in the centre of the cell. However, the Ca^{2+} rise did not occur with equal timing or amplitude around the circumference of the cell. The earliest signals were observed as eliptical Ca^{2+} increases at discrete locations (see images at 8 ms in Fig. 1*Aa*, marked by the black arrowheads in the right hand column). These events presumably reflected Ca^{2+} sparks at the diadic junctions between junctional SR (containing RyRs) and the plasma membrane (containing VOCCs). At the peak of the response, the lateral diffusion and overlap of these signals resulted in a 'ring' of elevated Ca^{2+} beneath the sarcolemma (e.g. images captured at 32 ms in Fig. 1*Aa*). However, there were distinct inhomogeneities within the subsarcolemmal Ca^{2+} rise, such that significant Ca^{2+} gradients were even observed in regions spaced only a few micrometres apart (e.g. region marked by the red arrowhead in Fig. 1*Aa*). A more quantitative representation of the Ca^{2+} concentration gradients observed during field stimulation of the same cell is illustrated by the traces in Fig. 1*Ab*. The outline of the cell is depicted by the inset image, and coloured circles mark the subcellular regions in which Ca^{2+} was monitored. The first regions to show Ca^{2+} rises had a lag time of less than 8 ms and reached maximal amplitude within 24 ms (red circle and corresponding red trace in Fig. 1*Ab*). Such regions were denoted 'eager sites' due to their ability to respond most rapidly. Between the eager sites were regions that exhibited weak regenerative Ca^{2+} responses (black circle and corresponding black trace in Fig. 1*Ab*).

Such 'failure sites', although immediately adjacent to eager sites, gave only slowly developing Ca^{2+} signals with ~25% of the amplitude of neighbouring regions. The centre of the cells typically gave a low-amplitude Ca^{2+} rise of ~200 nM (green circle and corresponding green trace in Fig. 1*Ab*). The spatially heterogeneous Ca^{2+} rise is also visible in the surface plots in Fig. 1*Ac*. The maximum response at 32 ms consisted of a discontinuous ring of peaks, with the centre of the cell showing a 'valley' of low Ca^{2+} concentration. Such Ca^{2+} gradients were typical for the majority of atrial myocytes paced in 1 mM Ca^{2+}-containing solution ($n > 100$), and were repetitively observed during a 1 Hz train of depolarisations (Fig. 1*Ad* and *e*). Since Ca^{2+} homeostatic and signalling mechanisms are steeply temperature dependent, we investigated the effect of increasing the temperature on the subcellular properties of Ca^{2+} signalling observed during E–C coupling.

The data depicted in Fig. 1*A* were obtained at 22°C, and the corresponding response of the same cell to depolarisation at 37°C is illustrated in Fig. 1*B*. Although the response was larger and more rapid in onset, and the 'ring' of elevated Ca^{2+} was more continuous, the Ca^{2+} rise was still restricted to the subsarcolemmal region (Fig. 1*Ba*). Furthermore, analysis of the Ca^{2+} signals at the same subcellular regions as in Fig. 1*A* revealed that the eager sites were generally at the same locations for both temperatures (Fig. 1*Ba*, marked by the black arrowheads in the right hand column).

Since the eager Ca^{2+} release sites were commonly activated within the 8 ms taken to acquire the first image after depolarisation (Fig. 1), we used confocal line scanning to obtain a better temporal resolution of the Ca^{2+} rise. Scanning along a subsarcolemmal region (Fig. 2*Aa*) revealed the rapid onset of eager sites at discrete regions within the cell (Fig. 2*Ab*). Between the eager sites, the Ca^{2+} signal rose more slowly (compare black and grey traces in Fig. 2*Ac*). Scanning through the centre of the same cell shows the slow development and low amplitude of the Ca^{2+} signal deeper within the cell (Fig. 2*Ad–f*).

The locations of eager and failure sites were the same for successive depolarisations, and were independent of the orientation of the cell relative to the stimulating electrodes. The line scan images in Fig. 2*Ba* depict the initiation of six sequential Ca^{2+} signals. Several eager sites can be distinguished in the line-scan images, with similar patterns of Ca^{2+} increase arising with each depolarisation. Although the same eager sites responded, one noticeable difference between them was that some sites had a consistent time course whilst others varied in their rise times. The traces in Fig. 2*Bb* depict the development of the Ca^{2+} signal at the locations marked by arrows in Fig. 2*Ba1*. One of the regions (black traces in Fig. 2*Bb*) showed little variation in its time course (< 1 ms difference for time to 10% peak in six trials), whilst at another site (grey traces in Fig. 2*Bb*) the latency before the rapid upstroke of the Ca^{2+} was more variable (~4–5 ms difference for time to 10% peak in six trials). Despite this variability, the activation order of the eager sites was on average the same with each depolarisation.

The consistent order of eager site recruitment is shown quantitatively in Fig. 3. The locations of 23 eager sites identified in an individual atrial myocyte are depicted on the cell image in Fig. 3*A*. The traces in Fig. 3*B* show the Ca^{2+} rise in three of the identified sites. To calculate the relative activation order of the 23 eager sites, the traces were expanded and the relative times at which each site reached 10% of its maximal eventual amplitude was estimated from the curves (see Methods), as illustrated in Fig. 3*C*. Using time to 10% of maximal amplitude minimises potential problems caused by diffusion of Ca^{2+} from neighbouring sites or motion artifacts during the contraction of the cell. Two-dimensional imaging, and not faster line scanning, was used to examine the activation order since eager sites around the circumference of a cell could be monitored. The first of the 23 eager sites to respond was always the site 'S' shown in Fig. 3*A*. The graph in Fig. 3*D* depicts the relative times, with reference to site S, taken for the Ca^{2+} signals at each eager site to reach 10% of their maximal amplitude. The data indicate that these eager sites responded in a consistent order, and that there was a ~10 ms delay in the development of the Ca^{2+} signal at different sites. In additional experiments, we observed that the order of activation for the eager sites did not depend on the orientation of the applied electrical field. Reversing the

field direction did not alter the activation sequence (data not shown). We tested whether the preferential activation of the eager sites was due to an intrinsically higher sensitivity to CICR. For this, we compared the eagerness of sites (i.e. relative latencies) and their ability to produce spontaneous Ca^{2+} sparks during rest. The correlation between eager sites and Ca^{2+} spark frequency is illustrated in Fig. 4. For the atrial myocyte shown, 14 subsarcolemmal Ca^{2+} release sites were analysed (Fig. 4*Aa*). These sites were found to have a reproducible order of activation (Fig. 4*Ab*; relative time taken to reach 10 % of peak amplitude; mean value of five consecutive stimulations) with a difference of up to 8 ms. Following termination of electrical pacing, a similar order was found when the frequency of spontaneous Ca^{2+} sparks was plotted (Fig. 4*Ac*). These data indicate that the most eager sites with the least lag times also displayed the highest frequency of spontaneous Ca^{2+} release events.

Since localised Ca^{2+} release events can appear to have slower onset if they are out of focus, we were concerned that our

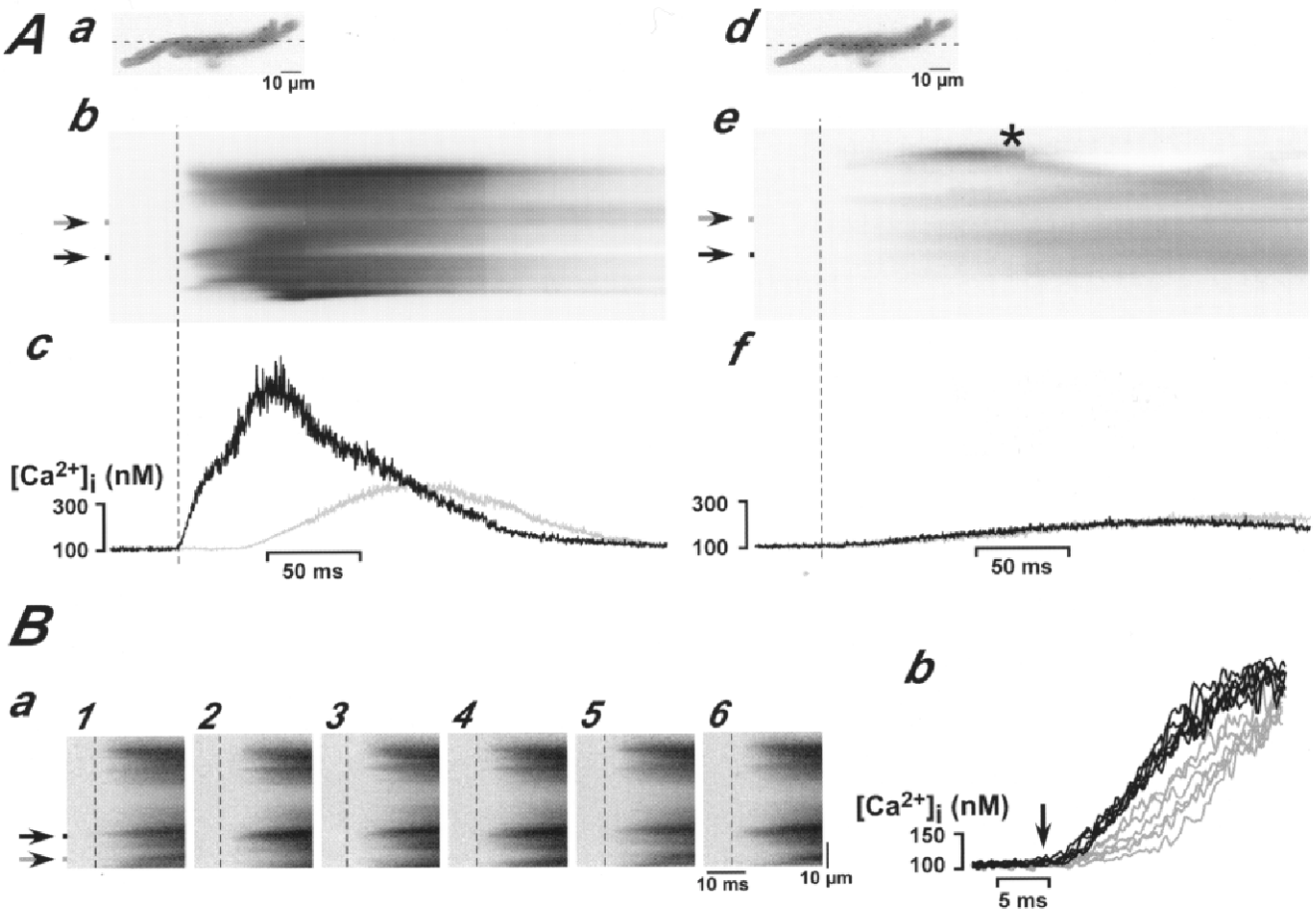

Figure 2. Spatial and temporal stability of eager Ca^{2+} spark sites

A depicts the development of Ca^{2+} signals in the subsarcolemmal (*Aa–c*) and central (*Ad–f*) regions of the same atrial myocyte using confocal line scanning. The positions of the scanned lines are depicted on the cell images in *Aa* and *Ad*. For *Ab* and *Ae*, time runs from left to right and the spatial dimension of the scanned line is vertical (the scanned line was turned 90 deg anticlockwise). The development of the Ca^{2+} signals along the regions indicated by the black and grey arrows is illustrated by the correspondingly coloured traces in *Ac* and *Af* (the bars to the right of the arrows indicate the segment that was averaged along the scanned line). The asterisk in *Ae* indicates a Ca^{2+} spark that occurred at the right boundary of the cell, while the left end of the cell (lower end of the line scan image) indicates a failure to elicit SR Ca^{2+} release. Due to the modest contraction of the cell, both *Ab* and *Ae* show movement artifacts visible as curvature of the edges of the plots. The dashed vertical lines in *Ab* and *Ae* indicate the time of field stimulation. Traces in panel *A* were representative for six cells from three rat hearts. *B* illustrates the reproducible recruitment of eager Ca^{2+} sparks sites with a train of six successive depolarisations. The images in *Ba1–6* depict individual line scans for each depolarisation. The dashed vertical lines mark the time of stimulation. The traces in *Bb* indicate the time course of the Ca^{2+} responses with each depolarisation at the regions marked by the black and grey arrows in *Ba1*. Similar results were obtained in five atrial cells from three hearts.

observation of eager sites and their predetermined activation order reflected Ca^{2+} release at different focal planes within the myocytes. To address this issue, the activation order of 11 Ca^{2+} release sites within a single atrial myocyte (Fig. 4*Ba*) was monitored at three focal planes differing by 0·5 μm. The sequence in which the Ca^{2+} release sites were activated was similar at each plane, although the absolute values varied slightly (Fig. 4*Bb*). These data indicate that

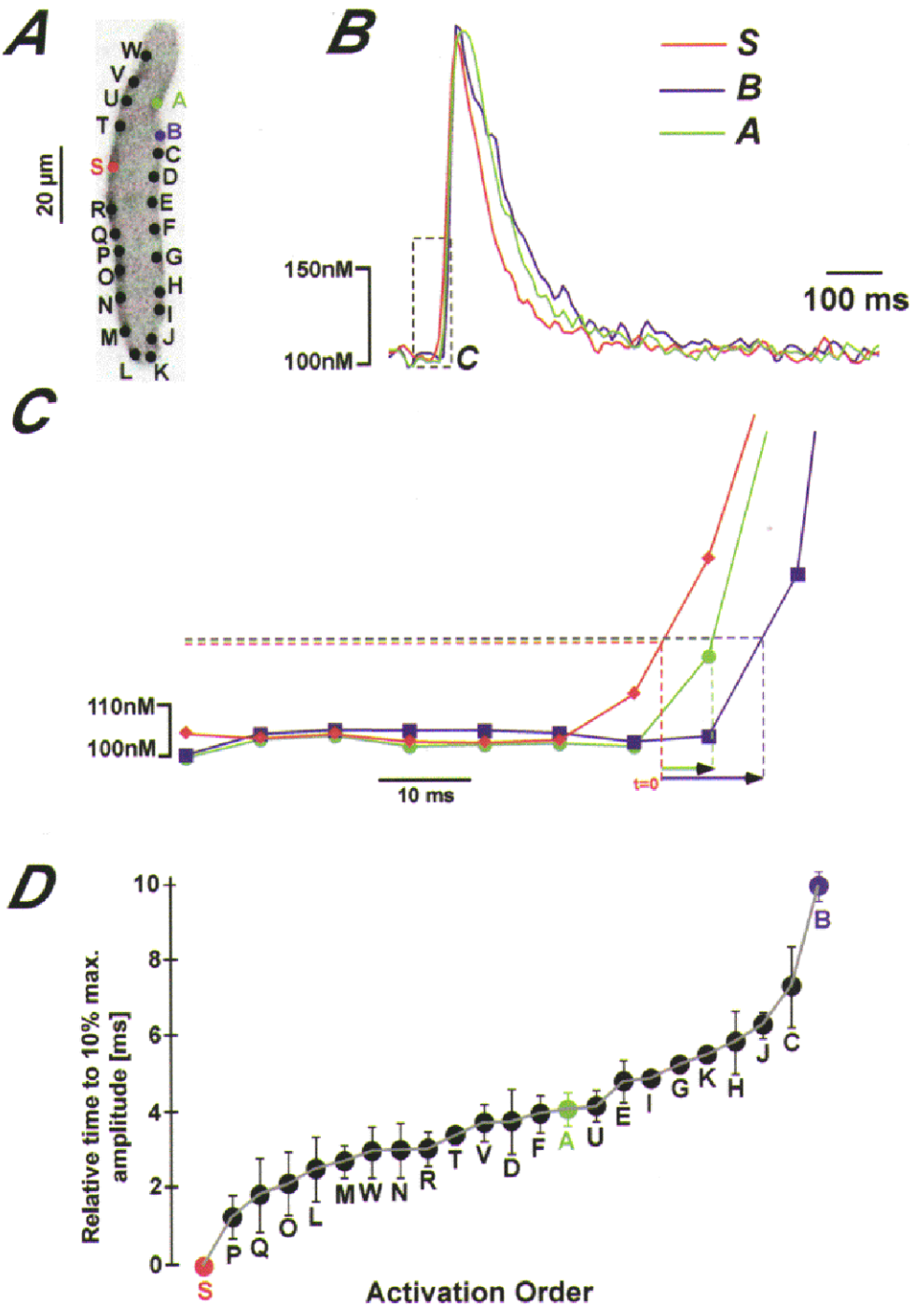

Figure 3. Reproducible activation order of eager sites

The relative activation times of the 23 eager sites depicted in *A* were analysed. Example traces from three of the eager sites are shown in *B*. To calculate the activation order of the eager sites, the time taken for the signals to reach 10 % of maximal amplitude (demarked by the horizontal dashed lines) was calculated as illustrated in *C*. The average delay of each eager site to respond after site 'S' is plotted in D (mean ± S.E.M. of 6 stimulations). Similar results were found in four additional myocytes from two hearts.

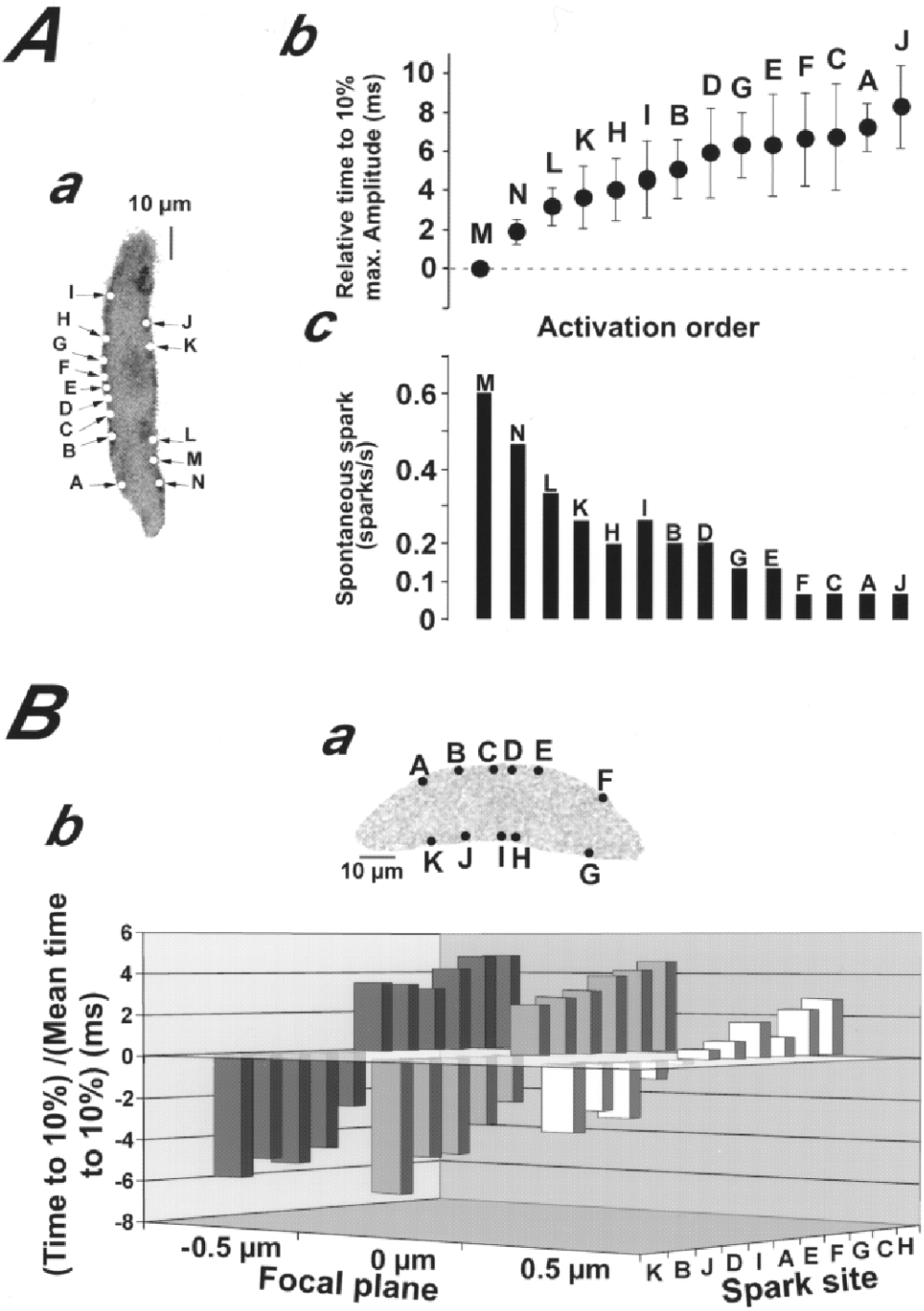

Figure 4. Properties of eager sites in rat atrial myocytes

Aa depicts a single atrial myocyte in which 14 discrete eager sites were identified. The relative activation order of these sites was calculated as described in the text, and is plotted in *Ab*. The bar graph in *Ac* shows the frequency of spontaneous Ca^{2+} sparks arising at the eager sites during 15 s in which the cell was not electrically stimulated. To assess Ca^{2+} spark frequency, the fluorescence images (collected at 120 Hz) were individually inspected for the appearance of new Ca^{2+} spark events. The relative activation order and degree of spontaneous activity were analysed in four additional myocytes from two rat hearts with similar results. *B* illustrates that the activation order of eager sites was not a result of different diffusion times for Ca^{2+} release sites out of focus into the confocal plane. The cell image in *Ba* depicts the 11 identified eager sites. The relative order of activation of these sites at three confocal planes differing axially by 0·5 μm is shown in *Bb*. A similar behaviour was found in three additional myocytes from two rat hearts.

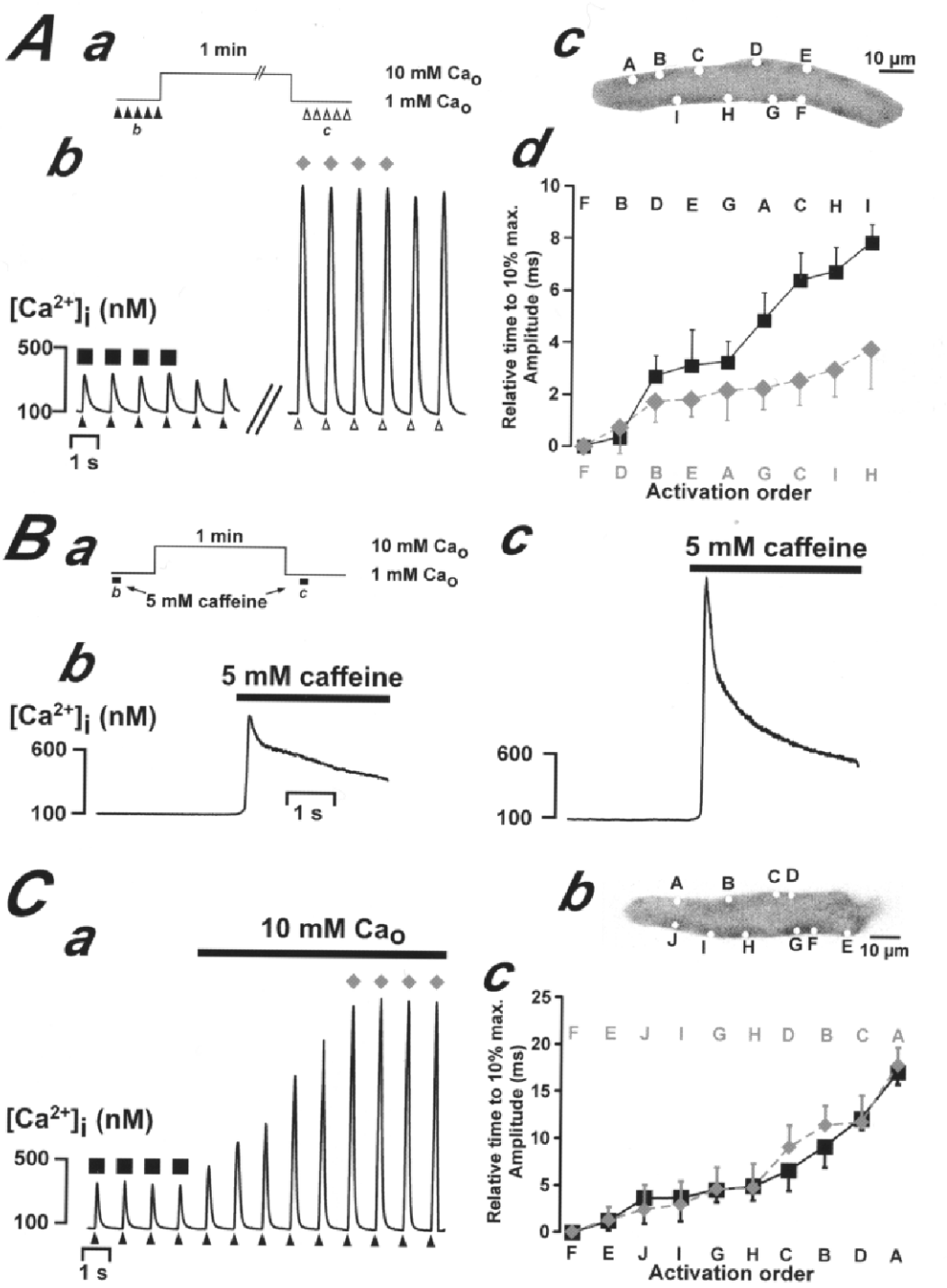

Figure 5. Enhanced SR Ca^{2+} load and Ca^{2+} influx did not change the activation order of eager sites

Aa depicts the experimental protocol used to increase the SR Ca^{2+} load. The arrowheads indicate the times at which electrical stimulation was given (1 Hz frequency). *Ab* illustrates Ca^{2+} transients before (black squares) and after (grey diamonds) the 1 min incubation in medium containing 10 mM Ca^{2+}. The arrowheads below the traces indicate the times of electrical stimulation. The white circles on the cell images in *Ac* depict the position of nine identified eager sites within the cell. The activation order of these sites under control conditions (black squares) and after the 1 min incubation in medium containing 10 mM Ca^{2+} (grey diamonds) is shown in *Ad*. For both the control and 10 mM Ca^{2+} conditions, the relative delays of the eager sites during four transients was averaged (marked by corresponding symbols above the traces in *Ab*). A similar behaviour was found in two additional myocytes. *B* depicts the typical increase in SR Ca^{2+} load caused by the 1 min incubation in 10 mM Ca^{2+} containing medium. *Ba* depicts the experimental protocol used. The Ca^{2+} responses evoked by superfusion with 5 mM caffeine before and after the 10 mM Ca^{2+} treatment are shown in *Bb* and *Bc*, respectively. *C* illustrates the effect of acutely increasing the

the observed order of activation of the Ca^{2+} signals was not due to different positions of the Ca^{2+}release sites relative to the confocal image plane.

We examined whether increasing the SR Ca^{2+} load or Ca^{2+} influx determined the position and activation order of the eager sites. The SR Ca^{2+} load was increased by bathing atrial myocytes in extracellular medium containing 10 mM Ca^{2+} concentration for 1 min, a procedure that typically enhances Ca^{2+} influx and store loading. The experimental protocol is schematically illustrated in Fig. 5*Aa*. Essentially, the responses of cells paced at 1 Hz in 1 mM Ca^{2+}-containing medium were compared before and after incubation in 10 mM Ca^{2+}. In the example shown in Fig. 5*A*, the global amplitude of the electrically evoked Ca^{2+} transients was increased by ∼500 % following the 10 mM Ca^{2+} treatment (Fig. 5*Ab*). This was essentially due to propagation of the Ca^{2+} signal throughout the cell, as reported by Hüser *et al.* (1996), in contrast to the largely subsarcolemmal response before altering SR Ca^{2+} load (data not shown). The activation order of nine eager sites identified in this cell (depicted in Fig. 5*Ac*) is shown in Fig. 5*Ad*. Incubation of the cells in 10 mM Ca^{2+} did not alter the location or activation order of the eager sites, although it did reduce the time interval between the sequential activation of the sites. The increased store load did not result in recruitment of extra eager sites in the observed confocal plane (data not shown). We confirmed that the 1 min incubation in 10 mM Ca^{2+} enhanced the Ca^{2+} load of the SR by directly activating the RyRs with caffeine. The experimental protocol for investigating the SR Ca^{2+} loading is depicted in Fig. 5*Ba*, which indicates that cells were superfused with caffeine either before or after the 10 mM Ca^{2+} treatment. The traces in Fig. 5*Bb* and *c* show that following the incubation in 10 mM Ca^{2+}, there was a substantial increase of SR Ca^{2+}.

Elevating the extracellular Ca^{2+} concentration from 1 to 10 mM during pacing significantly increased the amplitude of electrically evoked Ca^{2+} transients (Fig. 5*Ca*). Despite this acute change of extracellular Ca^{2+} concentration, the activation order of the ten eager sites depicted in Fig. 5*Cb* was unaffected (Fig. 5*Cc*). Similar to the situation where cells were incubated with 10 mM Ca^{2+} for 1 min (Fig. 5*A*), acutely increasing the extracellular Ca^{2+} concentration also changed the response from a largely subsarcolemmal 'ring' of Ca^{2+} to a globally regenerative response (data not shown). The data presented in Fig. 5 indicate that the location and activation order of eager Ca^{2+} release sites was unaffected by increasing either SR Ca^{2+} load or voltage-activated Ca^{2+} entry. Apart from decreasing the time interval between the activation of eager sites by an enhanced SR Ca^{2+} load (Fig. 5*A*), increasing extracellular Ca^{2+} had no effect on the early events of atrial myocyte E–C coupling.

The data described above illustrate that atrial myocytes display spatially heterogeneous Ca^{2+} signals upon depolarisation. Stereotypic responses are observed in the subsarcolemmal region, with variable amplitude Ca^{2+} transients in the central bulk of the cell. Within the subsarcolemmal region where the stereotypic Ca^{2+} rise occurs, there are substantial differences in the responsiveness of Ca^{2+} release sites, leading to an inhomogeneous subsarcolemmal Ca^{2+} signal. The mechanisms causing the Ca^{2+} release sites within an atrial myocyte to behave so distinctly are unclear. One plausible explanation would be a variable distribution of RyRs. Isolated atrial myocytes probed with a type II RyR-specific antibody generally displayed consistent distributions of immunoreactivity that did not allude to obvious reasons why Ca^{2+} release should fail at certain positions (Fig. 6*A*). Two regularly arranged populations of atrial RyRs were observed: junctional RyRs that underlie the initial subsarcolemmal Ca^{2+} elevation during E–C coupling and the non-junctional RyRs aligned along the SR within the centre of cells where the response is SR Ca^{2+}-load dependent (Fig. 6*Ab*). The only location where atrial myocyte RyRs appeared to be less regularly spaced was in a perinuclear region that was sometimes devoid of immunostaining (Fig. 6*A*; marked PR). A more detailed inspection of the immunostaining reveals that within both junctional and non-junctional RyR populations the channel distribution was punctate. Furthermore, between the junctional and non-junctional RyRs, there was a clear gap in the immunostaining of 0·5–1 μm that extended completely around the cell (marked by red lines in Fig. 6*Ab*). Ventricular myocytes also displayed regularly arranged RyRs (Fig. 6*B*). However, in contrast to atrial cells, the RyRs are all 'junctional' since they align the t-tubules that project into the cells (Fig. 6*Bb*).

To examine the functionality of the RyRs identified by immunostaining, caffeine (2·5 mM) was superfused onto atrial myocytes to directly activate the channels (Fig. 7). Irrespective of the external Ca^{2+} concentration or the SR Ca^{2+} load, application of caffeine evoked homogeneous Ca^{2+} signals that developed equally rapidly within the subsarcolemmal and central regions of the cells. Figure 7 depicts the response of a cell paced at 1 Hz in 1 mM Ca^{2+}-containing medium

extracellular Ca^{2+} concentration whilst the cells were electrically paced (the arrowheads beneath the trace in *Ca* indicate when depolarising pulses were applied; 1 Hz frequency). The white circles on the cell images in *Cb* depict the position of 10 identified eager sites within the cell. The activation order of these sites under control conditions (black squares) and after extracellular Ca^{2+} to 10 mM (grey diamonds) is shown in *Cc*. For both the control and 10 mM Ca^{2+} conditions, the relative delays of the eager sites during four transients was averaged (marked by corresponding symbols above the traces in *Ca*).

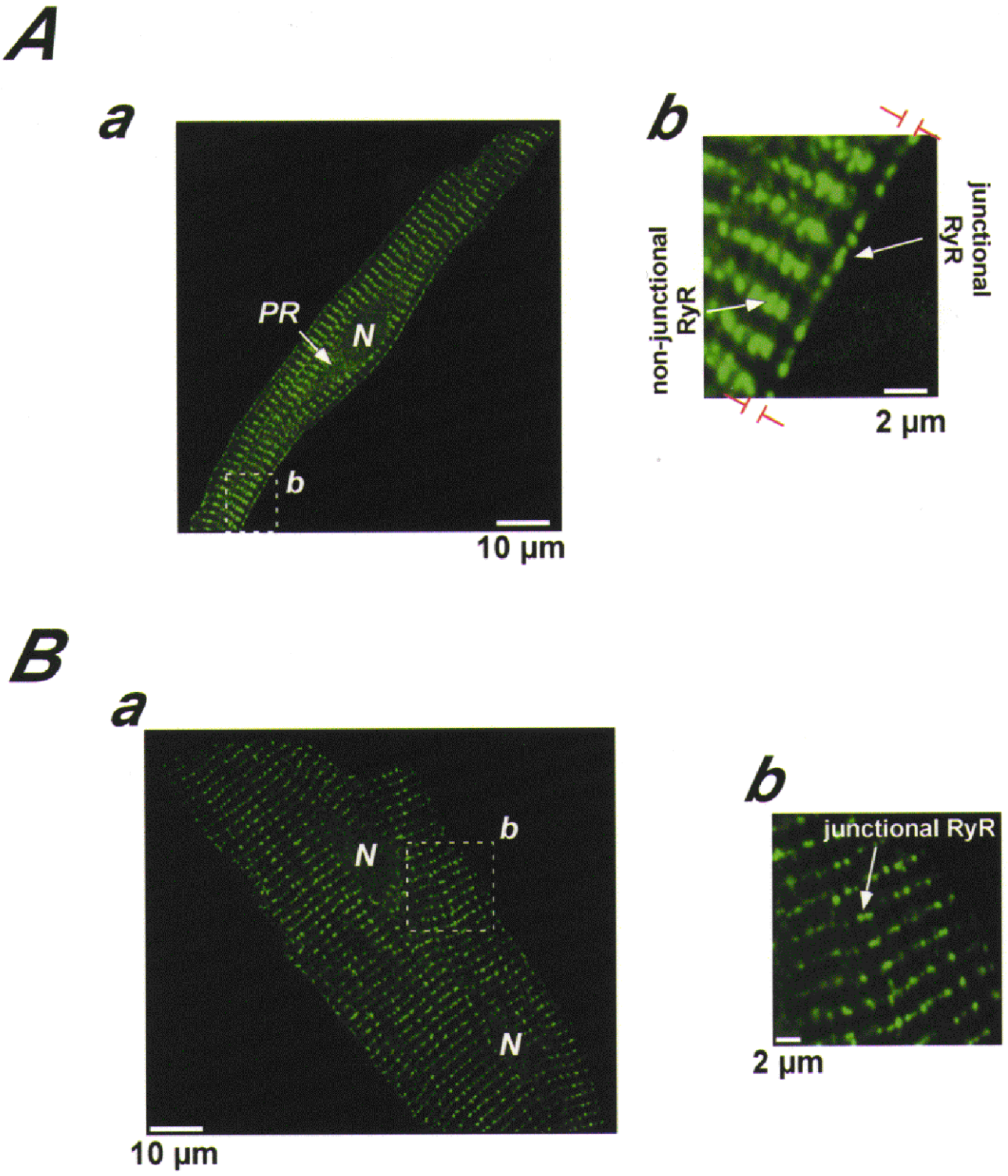

Figure 6. Immunolocalisation of type II RyRs in atrial and ventricular myocytes

A and *B* depict type II RyR immunostaining of single atrial and ventricular myocytes, respectively. In *Aa*, PR denotes the perinuclear region. For *Aa* and *Ba*, N indicates the position of the nuclei. The regions bounded by dashed box (*b*) in *Aa* and *Ba* are expanded in *Ab* and *Bb*, to show more clearly the punctate RyR staining and the separation of junctional and non-junctional RyRs in atrial cells.

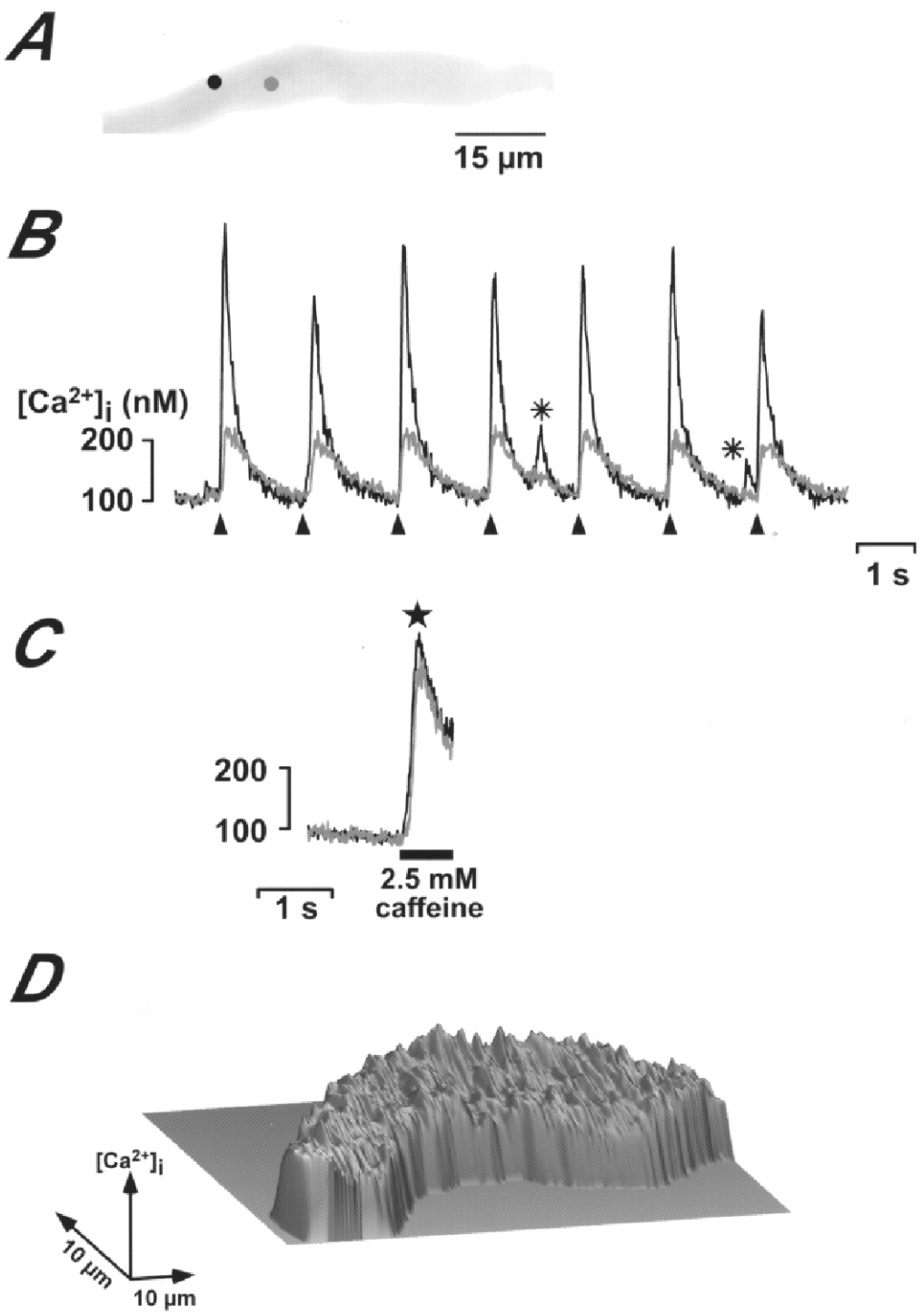

Figure 7. Caffeine, but not electrical depolarisation, evokes spatially homogeneous Ca^{2+} signals
Comparison of the spatial pattern of Ca^{2+} signals evoked by electrical depolarisation and caffeine. The cytosolic Ca^{2+} concentration was monitored at the two sites shown on the inset cell image in *A*. Electrical depolarisation (at 1 Hz frequency in 1 mM Ca^{2+} containing medium) evoked typically heterogeneous Ca^{2+} responses, with a larger Ca^{2+} increase in the subsarcolemmal regions (black trace in *B*) than in the centre of the cell (grey trace in *B*). The arrowheads denote the timing of the electrical pulses. *C* shows that application of caffeine to the same cell shortly after termination of the electrical pulses evoked Ca^{2+} signals with similar amplitudes and kinetics in both regions. The spatially homogeneous Ca^{2+} response to caffeine is illustrated by the surface plot in *D*, which shows the caffeine-induced Ca^{2+} response at the maximal amplitude. The asterisks in *B* represent spontaneous Ca^{2+} sparks.

where electrical pacing evoked typical Ca^{2+} signals with subsarcolemmal gradients and a poorly regenerative response in the central region of the cell (Fig. 7*B*). In contrast to the electrically evoked Ca^{2+} signals, with caffeine there was no evidence of subsarcolemmal gradients similar to those observed during pacing. Furthermore, the central bulk always responded with a Ca^{2+} signal of similar amplitude to that observed in the subsarcolemmal region (Fig. 7*C* and *D*).

DISCUSSION

The present study shows that within the Ca^{2+} response of atrial myocytes to electrical stimulation there is a consistent microscopic sequence of Ca^{2+} spark activation, along with regions that repeatedly fail to respond (Figs 1 and 2). Thus the spatially heterogeneous Ca^{2+} transient in an atrial myocyte is not stochastic, but is actually constructed from a predetermined recruitment of eager Ca^{2+} spark sites. Previous studies have reported that atrial myocyte E–C coupling is characterised by spatially heterogeneous Ca^{2+} signals (Berlin, 1995; Hüser *et al.* 1996). Due to the lack of t-tubules in atrial myocytes (Hüser *et al.* 1996), junctional couplings between VOCCs and RyRs only occur around the periphery of the cells (Sommer & Jennings, 1986; Lewis Carl *et al.* 1995; Lipp *et al.* 2000). For this reason, the Ca^{2+} rise is expected to be more rapid in subsarcolemmal regions (Figs 1 and 2; Berlin, 1995; Hüser *et al.* 1996). Our data indicate that the RyRs at the junctional couplings differ significantly in their 'eagerness' to activate during E–C coupling. The mechanisms underlying the eagerness of some Ca^{2+} release sites and the lack of responsiveness of others are unclear. Our immunostaining (Fig. 6*A*) and that of others (Lewis Carl *et al.* 1995) suggests that both RyRs and VOCCs are evenly distributed around the periphery of atrial myocytes. There are no apparent regions devoid of either RyRs (Fig. 6*A*) or VOCCs (Lewis Carl *et al.* 1995) that could explain the failure sites (Fig. 1) observed during Ca^{2+} responses. Nor are there any sites with apparently more RyRs or VOCCs that might underlie the eager sites. In addition, the occurrence of eager sites, their subcellular localisation and activation order also appeared to be independent of the SR Ca^{2+} load or Ca^{2+} influx. An alternative explanation is therefore that the functional coupling between RyRs and VOCCs at diadic junctions varies significantly, such that the Ca^{2+} influx signal is unable to trigger a regenerative release in some regions. Furthermore, the observation that spontaneous Ca^{2+} sparks occur most frequently at eager sites (Fig. 4*A*) suggests that there may be some intrinsic difference in RyR activity or sensitivity to CICR at those locations.

The principle of 'eager' Ca^{2+} release sites was initially suggested for skeletal muscle E–C coupling (Blatter *et al.* 1996), although it has not been widely reported. In smooth muscle cells, Ca^{2+} spark sites with a significantly higher rate of spontaneous activation have been observed, but it is unclear whether they also play a prominent role during electrical or hormonal stimulation of the cells (for review see Bolton *et al.* 1999). Similarly, in line-scan images of spontaneous Ca^{2+} sparks from unstimulated ventricular myocytes, it appears that only a few of the many Ca^{2+} spark sites show repeated activity, consistent with an intrinsic difference in RyR activation similar to that seen in the present study (Parker & Wier, 1997). However, for ventricular cardiomyocytes and skeletal muscle, it is more generally accepted that homogeneous Ca^{2+} rises occur during E–C coupling (for a review see Lipp & Niggli, 1996). Therefore in contrast to our observations with atrial myocytes, the potentially eager sites in ventricular and skeletal muscle are not apparent during E–C coupling.

Whereas the subsarcolemmal response can be considered as stereotypic, since it is unaffected by variations of temperature, SR Ca^{2+} load or Ca^{2+} influx, the central bulk of the atrial cell shows a response that is enhanced by greater SR Ca^{2+} load and Ca^{2+} influx (Fig. 5). The lack of central response from the cells (Fig. 1; see also Hüser *et al.* 1996), is surprising since the RyRs are regularly arranged throughout the major part of an atrial cell (Fig. 5; Lewis Carl *et al.* 1995; Lipp *et al.* 2000) with only the perinuclear regions showing less abundant RyR immunofluorescence. Furthermore, these RyRs within the central regions of atrial myocytes are functional and even under conditions of 1 Hz stimulation and 1 mM extracellular Ca^{2+} concentration the Ca^{2+} stores are substantially replete, since the RyR agonist caffeine causes a substantial homogeneous Ca^{2+} rise (Fig. 7).

Although there are no t-tubules to conduct the depolarisation deep into atrial myocytes, the subsarcolemmal Ca^{2+} rise is significant and could be expected to trigger CICR in deeper layers, so that a regenerative Ca^{2+} wave would sweep into the cells and cause a global Ca^{2+} increase (see Berlin, 1995; Hüser *et al.* 1996; Lipp *et al.* 1996*a*,*b*). Our data and those of Hüser *et al.* (1996) therefore indicate that with low SR Ca^{2+} loads the Ca^{2+} influx occurring during E–C coupling in atrial myocytes is only sufficient to trigger subsarcolemmal RyRs. The ~1 μM Ca^{2+} rise that follows is unable to activate significant CICR from RyRs that are less than a few micrometres away. To what degree the 1 μm gap between the junctional and non-junctional RyRs (see Fig. 6*A*), which was also described earlier by Lewis Carl *et al.* (1995), might be responsible for that failure remains unclear and needs further attention in the future.

In summary, atrial myocyte E–C coupling appears to occur as a predetermined sequence of Ca^{2+} spark recruitment. The sequential activation of eager sites and the lack of response from the failure sites produce a Ca^{2+} signal that is stereotypic for successive depolarisations in a single atrial myocyte. This predetermined nature of the atrial Ca^{2+} response might reflect variations in the microarchitecture of atrial diadic junctions or the intrinsic activation properties of RyRs.

Berlin, J. (1995). Spatiotemporal changes of Ca^{2+} during electrically evoked contractions in atrial and ventricular cells. *American Journal of Physiology* **38**, H1165–1170.

Berridge, M. J., Bootman, M. D. & Lipp, P. (1998). Calcium – a life and death signal. *Nature* **395**, 645–648.

Berridge, M. J., Lipp, P. & Bootman, M. D. (1999). Calcium signalling. *Current Biology* **9**, 157–159.

Berridge, M. J., Lipp, P. & Bootman, M. D. (2000). The versatility and universality of calcium signalling. *Nature Reviews Molecular Cell Biology* 1, 11–21.

Bers, D. M. (1991). *Excitation-Contraction Coupling and Cardiac Contractile Force*. Kluver Academic Publishers, Dordrecht.

Blatter, L. A., Tsugorka, A., Shirokova, N. & Rios, E. (1996). Eager triads in skeletal muscle: Heterogeneous distribution of voltage-elicited Ca^{2+} release revealed by confocal microscopy. *Biophysical Journal* **70**, 5 (abstract).

Bolton, T. B., Prestwich, S. A., Zholos, A. V. & Gordienko, D. V. (1999). Excitation-contraction coupling in gastrointestinal and other smooth muscles. *Annual Review of Physiology* **61**, 85–115.

Bootman, M. D. & Berridge, M. J. (1995). The elemental principles of calcium signalling. *Cell* **83**, 675–678.

Callewaert G. (1992). Excitation-contraction coupling in mammalian cardiac cells. *Cardiovascular Research* **26**, 923–932.

Cannell, M., Cheng, H. & Lederer, W. J. (1994). Spatial non-uniformities in $[Ca^{2+}]_i$ during excitation-contraction coupling in cardiac myocytes. *Biophysical Journal* **67**, 1942–1956.

Cheng, H., Lederer, W. J. & Cannell, M. B. (1993). Calcium sparks: elementary events underlying excitation-contraction coupling in heart cells. *Science* **262**, 740–744.

Fabiato, A. (1985). Time and calcium dependence of activation and inactivation of calcium-induced release of calcium from the sarcoplasmic reticulum of a skinned canine cardiac Purkinje cell. *Journal of General Physiology* **85**, 247–289.

Hüser, J., Lipsius, S. L. & Blatter, L. A. (1996). Calcium gradients during excitation-contraction coupling in cat atrial myocytes. *Journal of Physiology* **494**, 641–651.

Lewis Carl, S., Felix, K., Casswell, A. H., Brandt, N. R., Ball, W. J., Vaghy, P. L., Meissner, G. & Ferguson, D. G. (1995). Immunolocalization of sarcolemmal dihydropyridine receptor and sarcoplasmic reticular triadin and ryanodine receptor in rabbit ventricle and atrium. *Journal of Cell Biology* **129**, 673–682.

Lipp, P., Hüser, J., Pott, L. & Niggli, E. (1996*a*). Spatially non-uniform Ca^{2+} signals induced by the reduction of transverse tubules in citrate-loaded guinea-pig ventricular myocytes in culture. *Journal of Physiology* **497**, 589–597.

Lipp, P., Hüser, J., Pott, L. & Niggli, E. (1996*b*). Subcellular properties of triggered Ca^{2+} waves in isolated citrate-loaded guinea-pig atrial myocytes characterised by ratiometric confocal microscopy. *Journal of Physiology* **497**, 599–610.

Lipp, P., Laine, M., Tovey, S. C., Burrell, K., Li, W., Berridge, M. J. & Bootman, M. D. (2000). Functional IP_3 receptors that may modulate excitation-contraction coupling in the heart. *Current Biology* **10**, 939–942.

Lipp, P. & Niggli, E. (1994). Modulation of Ca^{2+} release in neonatal cultured rat cardiac myocytes: Insight from subcellular release patterns revealed by confocal microscopy. *Circulation Research* **74**, 979–990.

Lipp, P. & Niggli, E. (1996). A hierarchical concept of cellular and subcellular Ca^{2+}-signalling. *Progress in Biophysics and Molecular Biology* **65**, 265–296.

Lipp, P., Pott, L., Callewaert, G. & Carmeliet, E. (1990). Simultaneous recording of Indo-1 fluorescence and Na^+/Ca^{2+} exchange current reveals two components of Ca^{2+}-release from sarcoplasmic reticulum of cardiac atrial myocytes. *FEBS Letters* **275**, 181–184.

López-López, J., Shacklock, P., Balke, C. & Wier, W. (1995). Local calcium transients triggered by single L-type calcium-channel currents in cardiac cells. *Science* **268**, 1042–1045.

Minta, A., Kao, J. P. Y. & Tsien, R. Y. (1989). Fluorescent indicators for cytosolic calcium based on rhodamine and fluorescein chromophores. *Journal of Biological Chemistry* **264**, 8171–8178.

Parker, I. & Wier, W. G. (1997). Variability in frequency and characteristics of Ca^{2+} sparks at different release sites in rat ventricular myocytes. *Journal of Physiology* **505**, 337–344.

Sommer, J. R. & Jennings, R. B. (1986). The ultrastructure of cardiac muscle. In *The Heart and Cardiovascular System*, ed. Fozzard, H. A., Haber. E., Jennings, R. B., Katz, A. M. & Morgan, H. E., pp. 61–100. Raven Press, New York.

Sugiyama, T., Furuya, A., Monkawa, T., Yamamotohino, M., Satoh, S., Ohmori, K., Miyawaki, A., Hanai, N., Mikoshiba, K. & Hasegawa, M. (1994). Monoclonal-antibodies distinctively recognizing the subtypes of inositol 1,4,5-trisphosphate receptor – application to the studies on inflammatory cells. *FEBS Letters* **354**, 149–154.

Acknowledgements

This work was supported by the BBSRC, and by the MRC (grant no. G9808149). L.M. is an MRC student. M.D.B. is supported by a Royal Society University Research Fellowship.

Corresponding author

M. D. Bootman: Laboratory of Molecular Signalling, The Babraham Institute, Babraham, Cambridge CB2 4AT and Department of Zoology, University of Cambridge, Downing Street, Cambridge CB2 3EJ, UK.

Email: martin.bootman@bbsrc.ac.uk